DEUTSCHES ELEKTRONEN-SYNCHROTRON DESY

DESY 84-039
WIS-14/84-Ph April
May 1984

# F MESON PRODUCTION FROM $e^+e^-$ ANNIHILATION IN THE TASSO DETECTOR

by

*TASSO Collaboration*

ISSN 0418-9833

NOTKESTRASSE 85 · 2 HAMBURG 52

To be sure that your preprints are promptly included in the
HIGH ENERGY PHYSICS INDEX ,
send them to the following address ( if possible by air mail ) :

DESY
Bibliothek
Notkestrasse 85
2 Hamburg 52
Germany

DESY 84-039
WIS-14/84-Ph April
May 1984

ISSN 0418-9833

# F MESON PRODUCTION FROM $e^+e^-$ ANNIHILATION IN THE TASSO DETECTOR

TASSO Collaboration

presented by

U. Karshon

Department of Nuclear Physics, Weizmann Institute of Science, Rehovot, Israel

ABSTRACT

Inclusive $D^{*\pm}$ and $F^{\pm}$ production have been observed by $e^+e^-$ annihilation at high energies in the final states $D^0\pi^{\pm}$ and $\phi\pi^{\pm}$ respectively. The $D^{*\pm}$ energy spectrum is hard, peaking near x=0.6, and the $F^{\pm}$ spectrum is similar. The mass of the $F^{\pm}$ meson is 1975±9±10 MeV and its width is consistent with the mass resolution. The yield of $F^{\pm}$ production relative to $\mu$ pair production times the $\phi\pi^{\pm}$ branching ratio is $R_F \cdot B(F^{\pm}\to\phi\pi^{\pm}) = 0.064\pm0.013\pm0.019$. A preliminary upper limit for the $\phi 3\pi$ decay mode is $R_F \cdot B(F^{\pm}\to\phi\pi^{\pm}\pi^{+}\pi^{-})<0.025$ (90% C.L.)

Talk presented at the XIX Rencontre de Moriond, La Plagne-Savoie-France, March 4-10, 1984



## 1. Introduction and experiment

### a) Charmed meson production

The most abundant production of multi-hadronic final states in $e^+e^-$ collisions at high energies is by the two-jet mechanism, which originates from a quark-antiquark creation via one-photon annihilation: $e^+e^-\to\gamma^*\to q\bar{q}\to$hadrons. At PETRA energies, five quark pairs can be produced in a ratio proportional to the square of the quark charges $u\bar{u}:d\bar{d}:s\bar{s}:c\bar{c}:b\bar{b} = 4:1:1:4:1$. On the other hand, the ratio of "sea" quark pairs in the hadronization process is roughly given by $u\bar{u}:d\bar{d}:s\bar{s}:c\bar{c}:b\bar{b} = 1:1:0.4:0:0$, where the 0.4 is estimated from the experimental inclusive $K/\pi$ ratio in the TASSO data[1] and, at PETRA energies, the excitation of heavy ($c\bar{c}$ and $b\bar{b}$) "sea" pairs is negligible. Consequently, charm production is copious and occurs in 36% of the two-jet events, and the charmed hadrons are associated with primary c-quarks. The charm-strange meson $F^+(=c\bar{s})$ is expected to be produced with a cross-section of $\sim 0.4$ times that of the $D^+$ $(=c\bar{d})$ meson.

The mechanism of heavy quark fragmentation (Q=c,b) into heavy mesons (H) has been qualitatively discussed by Bjorken and Suzuki[2], who argued that Q decelerates only slightly when forming the meson H with a "sea" antiquark $\bar{q}$. A more quantitative empirical form for the fragmentation function of a heavy quark has been recently derived by Peterson et al.[3]:

$$D_Q^H(x) \sim \frac{1}{x\left[1-\frac{1}{x}-\frac{\varepsilon_Q}{1-x}\right]^2}\,;\quad \varepsilon_Q \approx (M_{\bar{q}}/M_Q)^2 \qquad (1)$$

where $x = E_H/E_Q$ is the fractional energy of the heavy meson with respect to the heavy quark (or in the two-jet case with respect to the $e^{\pm}$ beam energy). Typical values for charm and bottom are[3] $\varepsilon_c=0.15$ and $\varepsilon_b=0.15\times(M_c/M_b)^2=0.016$.

### b) Charmed meson decay

The charmed mesons with the lowest mass (D and F) can decay only weakly. The most favorite decays are via a spectator diagram with the Cabibbo allowed transition c→s, such as shown in this page. Thus the decays $F^{\pm}\to\phi\pi^{\pm}$, $\eta\pi^{\pm}$, $\phi\rho^{\pm}$, $\eta\rho^{\pm}$ are expected to be important.

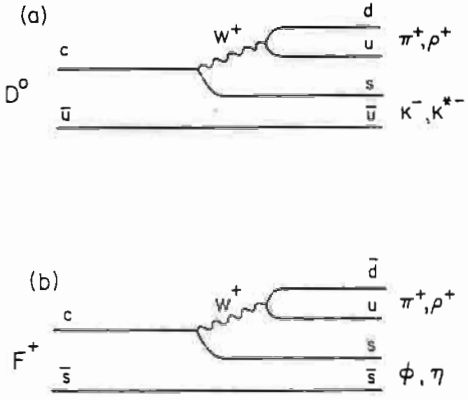

c) Event selection

The main components of the TASSO detector[4] used in the present analysis are the proportional and drift chambers and the time-of-flight (TOF) counters in the central detector. The event sample consists of 5.4 $pb^{-1}$ (5284 events) at low energies ($12 < W < 28$ GeV) and 77.6 $pb^{-1}$ (23882 events) at high energies ($29.5 < W < 42$ GeV with a weighted average $\bar{W} = 34.7$ GeV), where W is the total c.m. energy. The event selection of the multihadronic sample has been described previously[5]. The most important cuts for our analysis are : (1) At least 4 (5) accepted charged tracks for W = 12-26 GeV (W > 26 GeV). (2) The momentum sum $\Sigma|p_i|$ of the charged particle momenta had to be larger than 0.265 W. A momentum resolution for charged particles of $\sigma_p/p = 0.017 \cdot \sqrt{1+p^2}$ (p in GeV/c) was obtained (including multiple scattering). When the average beam position was included as a constraint in the track reconstruction, the momentum resolution improved significantly, yielding $\sigma_p/p = 0.010 \sqrt{2.9+p^2}$ (p in GeV/c). This inclusion is crucial for the study of heavy mesons, where particles are energetic due to the hard fragmentation function, as described earlier, and multiple scattering, interactions and decays are small. In order to improve the signal to noise ratio, strict cuts were imposed on the quality of the reconstructed "beam constraint" tracks.

## 2. $D^{*\pm}$ production

The scaled cross-section for the reaction $e^+e^- \to D^{*\pm}$+anything at $\bar{W}$=34.4 GeV, where the $D^{*\pm}$ is detected via the chain $D^{*\pm} \to D^0\pi^\pm$; $D^0 \to K^\mp\pi^\pm$ is shown in fig. 1 from the TASSO data[6] as well as from other experiments. The distribution is consistent with MARKII and HRS results and with the hard spectrum hypothesis[2-3]. The solid curve is a fit of the TASSO data to eq. (1) with $\varepsilon_c$=0.18±0.07. These results show that the $D^*$ carries a primary c quark.

## 3. $F^\pm$ production

a) Previous results

The strange-charm mesons ($F,F^*$) are much less known compared to the non-strange ones ($D,D^*$). The first possible $F^\pm$ signal has been reported in $e^+e^- \to F^\pm$+anything at W=4.42 GeV by the DASP collaboration[7]. They saw 6 events in the $\eta\pi^\pm$ decay mode and gave a mass of 2.03±0.06 GeV. Later, the OMEGA spectrometer group claimed to have seen F signals in $\gamma p \to F^\pm$+anything in various decay modes[8]. The F mass, averaged over all their measured decay modes, is 2.02±0.01 GeV. Recently, the CLEO group[9] reported a significant $F^\pm$ signal in $e^+e^- \to F^\pm$ + anything at W=10.5 GeV in the $\phi\pi^\pm$ decay mode with a mass of 1970±5±5 MeV, which is at variance with the OMEGA results.



b) Extraction of the $F^\pm$ signal

$F^\pm$ production was searched for[10] in the decay mode $F^\pm \to \phi\pi^\pm \to K^+K^-\pi^\pm$ with the hadronic events from all beam energies W (see chapter 1c). Particle identification in the TOF counters[11] was used to reduce the number of wrong mass assignments. As can be seen in fig. 2, the π/K separation with the TOF counters is possible for momenta p<1.0 GeV/c, while (π+K)/p separation is feasible up to p<1.4 GeV/c. If the $F^\pm$ energy spectrum is hard as that of the $D^{*\pm}$ (fig.1), then the φ, which carries most of the $F^\pm$ momenta, is also expected to be energetic. Therefore, $K^\pm$ identification in the TOF counters was not required in this analysis.

Candidates for φ mesons were searched for by looking at invariant mass combinations of oppositely charged tracks interpreted as kaons. However, particles positively identified as pions or protons by the TOF counters were not considered as kaons. To this end, probabilities $W_i$ were calculated for each particle type $i(i=\pi,K,p)$: $W_i = c \cdot f_i(p) \cdot \exp[-(\tau_m-\tau_i)^2/2\sigma_\tau^2]$, where $\tau_m$ is the measured TOF, $\tau_i$ the expected TOF for hypothesis i, $\sigma_\tau$ the resolution for the time measurement[11], $f_i(p)$ the momentum dependent particle fraction for the hypothesis[11], and c a normalization constant such that $\Sigma W_i$=1.0. A particle is called a sure pion, if $W_\pi$>0.9 for $0.3<p_\pi<1.0$ GeV/c; a sure kaon, if $W_K$>0.6 and $0.1<M^2<0.6$ GeV$^2$ for $0.3<p_K<1.0$ GeV/c; a sure proton, if $W_p$>0.6 and $M^2$>0.6 GeV$^2$ for $0.4<p_p<1.4$ GeV/c, where M is the mass of the particle, as calculated from the momentum and TOF measurements.

The $K^+K^-$ invariant mass spectrum is shown in fig. 3. A clear φ signal is seen for the combinations with a fractional energy $x_{KK}=2E_{KK}/W>0.4$ (shaded histogram). Fitting the latter distribution to a gaussian shape plus a background parametrized in terms of the $K^+$ momentum in the $K^+K^-$ rest frame times a polynomial, yields a mass (1023±2 MeV) consistent with the standard φ mass, and a FWHM width (21±7 MeV) consistent with the experimental resolution. In the following, all $K^+K^-$ mass combinations within ± 15 MeV of the nominal φ mass are defined as φ candidates.

Combining the φ candidates with any of the other charged tracks in the event, interpreted as a pion, where particles identified as sure kaons or protons by the TOF system were not included, the resulting $K^+K^-\pi^\pm$ mass spectrum is given in fig. 4. Combinations with a fractional energy $x_{KK\pi}=2E_{KK\pi}/W>0.4$ are shown in the full histogram and with $x_{KK\pi}>0.5$ in the shaded histogram. A clear peak is seen at a mass around 1.97 GeV. In order to find if this enhancement is associated with the φπ channel or with the large background under the φ (see fig. 3), we have looked at the following plots: 1. The $K^+K^-$ mass distribution for $K^+K^-\pi^\pm$ mass combinations in the "1.97 GeV" region ($1.94<M_{KK\pi}<2.02$ GeV; white histogram in fig. 5) and in a "control" region ($1.86<M_{KK\pi}<1.90$ GeV or $2.06<M_{KK\pi}<2.10$ GeV; shaded histogram in fig. 5). In order to reduce background, only combinations

with $X_{KK\pi}>0.5$ were considered. A clear excess is seen in the $\phi$ region for the "1.97 GeV" histogram compared to the "control" histogram. 2. The $K^+K^-\pi^\pm$ mass spectrum for $K^+K^-$ combinations in a "control $\phi$" region, defined to be close to the $\phi$ mass ($1.05<M_{KK}<1.10$ GeV), and with $X_{KK\pi}>0.4$, shows no signal in the "1.97 GeV" region (fig. 6b).

The mass and width of the signal are determined by fitting to the $K^+K^-\pi^\pm$ mass spectrum in the $\phi$ region a gaussian plus a background term of the form $dn/dM=a_o+a_1M+a_2M^2$ (fig. 6a). The fit yielded 49±14 events in the signal and a mass of 1975±9 (stat.)±10 (syst.) MeV. The systematic uncertainty ($\leq$ 10 MeV) was determined from the $\phi$ peak position, from $K^o_s\to\pi^+\pi^-$ decays, and from measuring the total c.m. energy with muon pairs. The fitted width of the gaussian is 64±21 MeV (FWHM), consistent with the expected mass resolution. The mass, width and $\phi\pi$ decay mode of the "1.97 GeV" enhancement are in agreement with the F signal of CLEO[9].

c) $F^\pm$ energy spectrum and cross section

For cross section determination, $F^\pm$ production is further studied only at high energies W>29.5 GeV ($\bar{W}$=34.7 GeV). The $K^+K^-\pi^\pm$ mass distribution for the $\phi$ candidates has been fitted for various $X_{KK\pi}$ intervals between 0.3 and 1.0 with a polynomial background plus a gaussian for the $F^\pm$. The overall detection efficiency for the F meson has been computed from Monte-Carlo generated events of the type

(a) $e^+e^-\to c\bar{c}$; (b) $c(\text{or }\bar{c})\to F^\pm$; (c) $F^\pm\to\phi\pi^\pm$; (d) $\phi\to K^+K^-$. (2)

Detector acceptance, gluon emission, radiative effects and the event selection criteria were included in the Monte-Carlo simulation. In (2c) an isotropic distribution was assumed for the $\pi^\pm$ in the $\phi\pi$ rest frame, and the decay (2d) was generated with a $\cos^2\theta_K$ distribution, where $\theta_K$ is the angle between the $K^+$ in the $\phi$ rest frame and the $\phi$ direction in the $\phi\pi$ rest frame. The resulting efficiency varies in the range $0.3<X_{KK\pi}<0.9$ between 0.46 and 0.26 with an average of 0.31.

In fig. 7, the $F^\pm$ scaled cross section times the $\phi\pi$ branching ratio, $\frac{s}{\beta}\cdot d\sigma/dx\cdot B(F^\pm\to\phi\pi^\pm)$, is shown as a function of the scaled F energy $x=2E_F/W$, where $s=W^2$, $\beta=p_F/E_F$, and the other decay modes of the $\phi$ are included, assuming[12] $B(\phi\to K^+K^-)=0.49\pm0.01$. The errors are statistical only and do not include overall systematic uncertainties of ±30% due to detection efficiency and background determination. The shape of the distribution in fig. 7 is similar to that of the $D^*$ cross section (fig. 1) and is described well by the parametrization of eq.(1). A fit to the data of fig. 7 (solid curve) yielded $\varepsilon=0.45\pm0.25$, compared to the value of 0.18±0.07 obtained in chapter 2 for $D^*$ production. This consistency with a hard fragmentation is a further evidence that our signal is indeed the F-meson.

Integrating over all the measured range (x>0.3), the $F^\pm$ cross section



relative to the $\mu$ pair cross section ($\sigma_{\mu\mu}=4\pi\alpha^2/3s=0.072$ nb at 34.7 GeV), $R_F\equiv\sigma_F/\sigma_{\mu\mu}$, times the $\phi\pi$ branching-ratio is given by $R_F(x>0.3)\cdot B(F^\pm\to\phi\pi^\pm)$ = 0.061±0.012±0.018. Extrapolating with the parametrization (1) to the range x<0.3, the total $F^\pm\to\phi\pi^\pm$ production is $R_F\cdot B(F^\pm\to\phi\pi^\pm)$ = 0.064±0.013±0.019.

d) Estimation of the $F^\pm\to\phi\pi^\pm$ branching ratio

The total yield for primary strange-charm meson production is expected to be $R(c\bar{s}+\bar{c}s)$ = 4.01 x (4/11)x2x0.167=0.486, where 4.01 is the measured total R value[5], 4/11 is the relative contribution of the c quark to R, 2 stands for the 2-jets, and 0.167 is the assumed probability to obtain an $s\bar{s}$ pair from the "sea".[1] With these assumptions we obtain a branching ratio $B(F^\pm\to\phi\pi^\pm)=0.13\pm0.03\pm0.04$, compared to the value $\sim$ 0.044 of ref. 9). The systematic error includes only the uncertainties in the measured cross section. This result may be smaller by $\lesssim$ 25% due to possible F production at low x from primary b quarks.

e) Upper limit for the $F^\pm\to\phi\pi^\pm\pi^+\pi^-$ decay mode

Preliminary results of the ARGUS collaboration[13] yield a similar $F^\pm\to\phi\pi^\pm$ signal at a mass of 1974±4 MeV. In addition, they see a less significant enhancement at 1967±3 MeV in the channel $F^\pm\to\phi\pi^\pm\pi^+\pi^-$. We have looked for an $F^\pm$ signal in the $\phi\pi^\pm\pi^+\pi^-$ effective mass and found none. Using Monte-Carlo generated events of the type: $e^+e^-\to c\bar{c}$; $c(\text{or }\bar{c})\to F^\pm$; $F^\pm\to\phi\pi^\pm\pi^+\pi^-$; $\phi\to K^+K^-$ with isotropic F and $\phi$ decays, the experimental resolution of an $F^\pm$ signal is $\Gamma$=51 MeV (FWHM) and the overall efficiency for $x_{\phi3\pi}=2E_{\phi3\pi}/W>0.4$ is $\sim$0.12. The $\phi\pi^\pm\pi^+\pi^-$ mass spectrum for $x_{\phi3\pi}>0.4$ is shown in fig. 8. This distribution was fitted to a background term of the form $\frac{dn}{dM}=a\cdot\exp(bM)$ plus a gaussian with a fixed mass (1.97 GeV) and width (51 MeV) (solid curve in fig. 8). A preliminary upper limit for $F^\pm\to\phi\pi^\pm\pi^+\pi^-$ production from this fit is: $R_F\cdot B(F^\pm\to\phi\pi^\pm\pi^+\pi^-)<0.023$ (90% C.L.). With the same assumption on $R_F$ as in chapter 3d, a preliminary upper limit for the $\phi3\pi$ branching ratio of the $F^\pm$ is: $B(F^\pm\to\phi\pi^\pm\pi^+\pi^-)<0.048$ (90% C.L.).

4. Conclusions

The charmed meson $D^{*\pm}$ is produced in $e^+e^-$ annihilation at $\bar{W}$=34.4 GeV with a hard spectrum, as expected from the formulation of Peterson et al.[3] (eq.1). The average fractional energy of the $D^*$ is $\bar{x}=0.57\pm0.04$.

The strange charm meson $F^\pm$ is detected in the final state $\phi\pi^\pm$ with a mass of 1975±9±10 MeV and a width consistent with the experimental resolution. The x-dependence of the scaled cross section of the $F^\pm$ is similar to that of the $D^{*\pm}$. The contribution of the measured $F^\pm$ production to the total hadronic cross section times the $\phi\pi^\pm$ branching ratio is $R_F(x>0.3)\cdot B(F^\pm\to\phi\pi^\pm)$ = 0.061±0.012±0.018. Assuming an x-dependence as in eq.(1), no contribution from b-quarks and a ratio of "sea" quark pairs given by $u\bar{u}:d\bar{d}:s\bar{s}=1:1:0.4$, the $\phi\pi^\pm$ branching ratio is

$B(F^{\pm}\to\phi\pi^{\pm})=0.13\pm0.03\pm0.04$. With similar assumptions, a preliminary upper limit for the $\phi 3\pi$ branching ratio is $B(F^{\pm}\to\phi\pi^{\pm}\pi^{+}\pi^{-})<0.048$ (90% C.L.).

References:


1. TASSO Collaboration, M. Althoff et al., Phys. Lett. 130B (1983) 340; TASSO Collaboration, M. Althoff et al., to be published.
2. J. D. Bjorken, Phys. Rev. D17 (1978) 171; M. Suzuki, Phys. Lett. 71B (1977) 139.
3. C. Peterson et al., Phys. Rev. D27 (1983) 105.
4. TASSO Collaboration, R. Brandelik et al., Z. Phys. C4 (1980) 87; Phys. Lett. 83B (1979) 261.
5. TASSO Collaboration, R. Brandelik et al., Phys. Lett. 113B (1982) 499.
6. TASSO Collaboration, M. Althoff et al., Phys. Lett. 126B (1983) 493.
7. DASP Collaboration, R. Brandelik et al., Phys. Lett. 80B (1979) 412.
8. D. Aston et al., Phys. Lett. 100B (1981) 91; Nucl. Phys. B189 (1981) 205; M. Atkinson et al., Z. Phys. C17 (1983) 1.
9. A. Chen et al., Phys. Rev. Lett. 51 (1983) 634.
10. TASSO Collaboration, M. Althoff et al., Phys. Lett. 136B (1984) 130.
11. TASSO Collaboration, R. Brandelik et al., Z. Phys. C17 (1983) 5.
12. Particle data group, Phys. Lett. 111B, April 1982.
13. R. Orr, these proceedings.




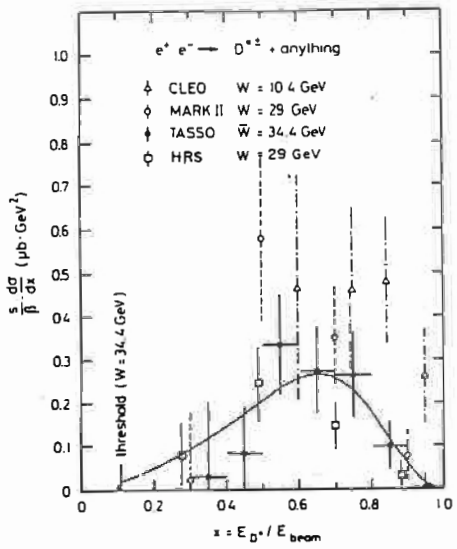


Fig. 1. The scaled cross section for $e^+e^- \to D^{*\pm} + X$ at $\bar{W}$=34.4 GeV. Errors are statistical only. Also shown are measurements from CLEO, MARK II and HRS. The curve is a fit to eq. (1) with $\varepsilon_c = 0.18\pm0.07$.

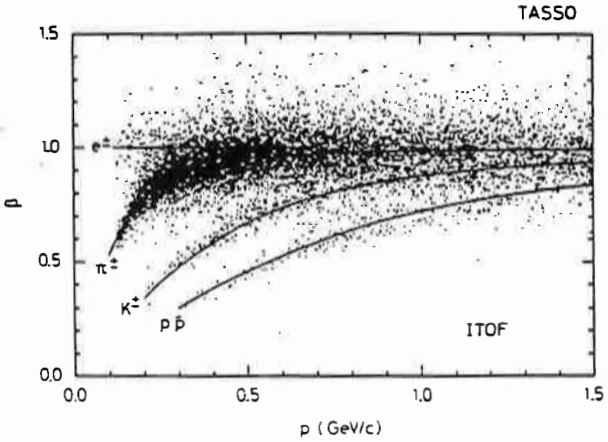


Fig. 2. Particle velocity β vs. momentum for tracks from multihadronic events using the TOF counters in the central detector.

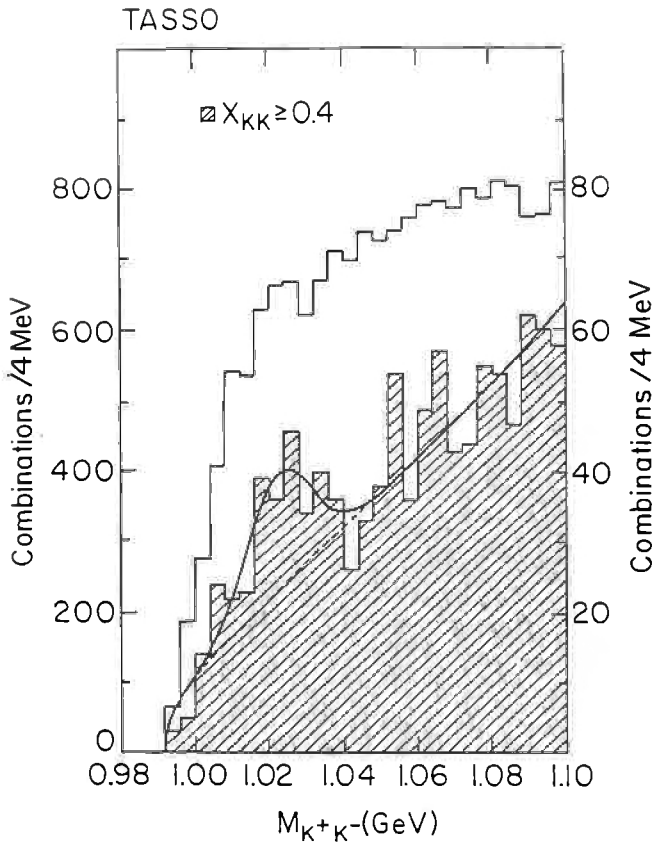


Fig. 3. Effective mass distribution of oppositely charged particles interpreted as kaons. The shaded histogram (right hand side scale) is for combinations with $x_{KK} > 0.4$. The curve is a fit to a gaussian $\phi$ resonance and a background term (see text).



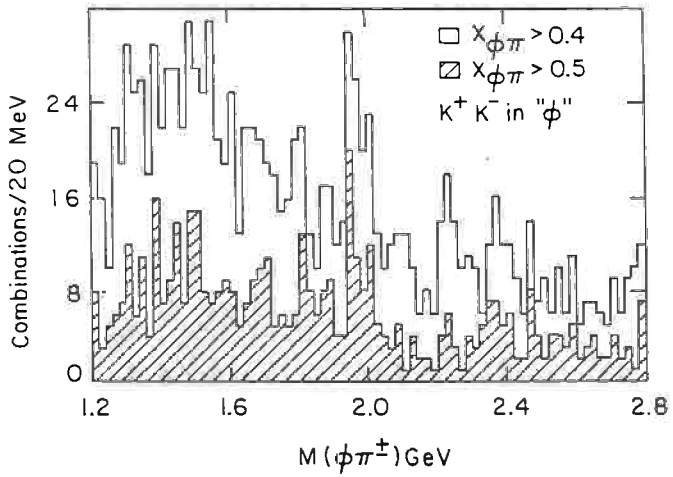


Fig. 4. Distribution of the $K^+K^-\pi^\pm$ effective mass with $x_{KK\pi} > 0.4$ (> 0.5 for the shaded histogram) for $K^+K^-$ combinations in the "$\phi$ region" ($1.005 < M_{K^+K^-} < 1.035$ GeV).

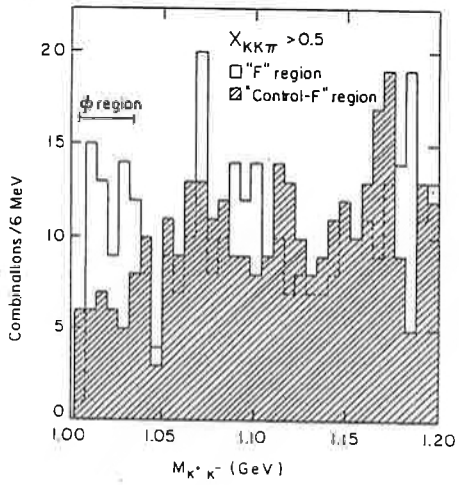


Fig. 5. The $K^+K^-$ mass distribution for $K^+K^-\pi^\pm$ effective mass combinations: white histogram - in the "F" region ($1.94 < M_{KK\pi} < 2.02$ GeV); shaded histogram - in a "control F" region ($1.86 < M_{KK\pi} < 1.90$ GeV or $2.06 < M_{KK\pi} < 2.10$ GeV). Only combinations with $x_{KK\pi} > 0.5$ are shown.

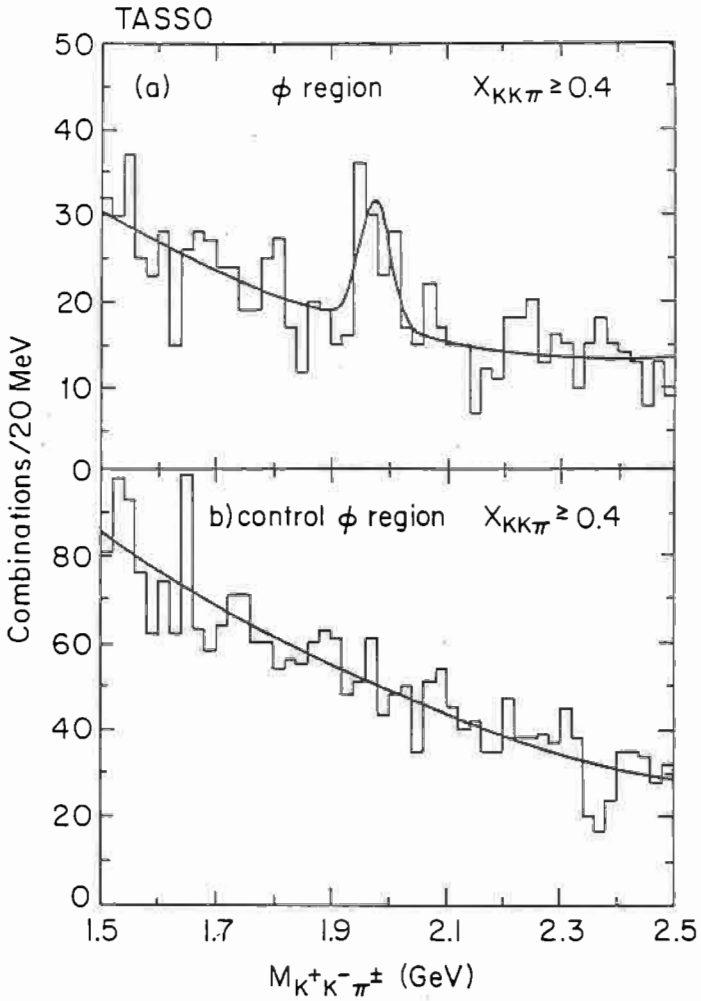


Fig. 6. Effective mass $K^+K^-\pi^\pm$ distributions with $x_{KK\pi} > 0.4$: a) For $K^+K^-$ combinations in the "φ region" ($1.005 < M_{K^+K^-} < 1.035$ GeV). The curve is a fit to a gaussian plus a background term (see text); b) For $K^+K^-$ combinations in a "φ control region" ($1.05 < M_{K^+K^-} < 1.10$ GeV). The curve is a fit to a smooth background.



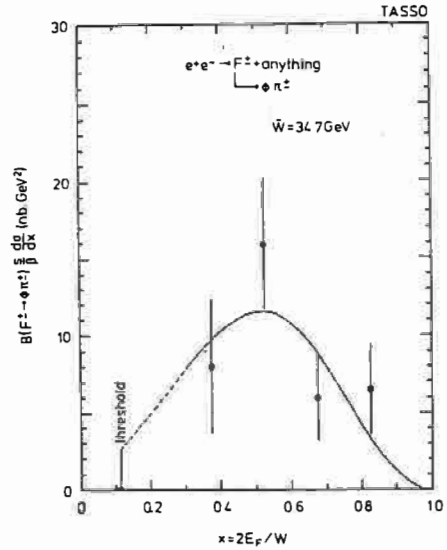


Fig. 7. The scaled cross section times the $\phi\pi^\pm$ branching ratio for $e^+e^- \to F^\pm + X$ at $\bar{W}$ = 34.7 GeV. Errors are statistical only. The curve is a fit to eq.(1) with $\varepsilon_c^* = 0.45 \pm 0.25$.

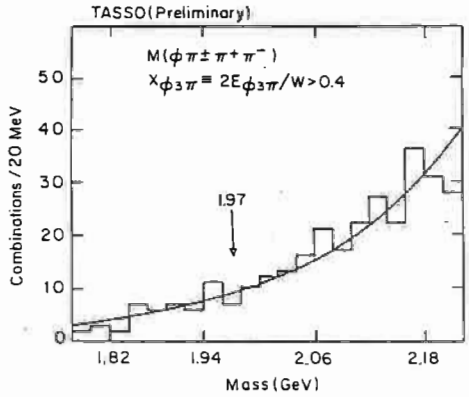


Fig. 8. Distribution of the $K^+K^-\pi^\pm\pi^+\pi^-$ effective mass with $x_{KK3\pi} > 0.4$ for $K^+K^-$ combinations in the "φ region" ($1.005 < M_{K^+K^-} < 1.035$ GeV). The curve is a fit to a gaussian at M=1.97 GeV plus a background term (see text).